

Neutron diffraction study of porous glasses structure

ALEXANDER NABEREZHNOV^{1, 4*}, TATIANA ANTROPOVA², ILYA GLAVATSKY³,
MAKSIM SEREGIN¹, IRINA DROZDOVA²

¹Ioffe Physical Technical Institute, Polytekhnicheskaya 26, 194021, Saint Petersburg, Russia

²Grebenshchikov Institute of Silicate Chemistry, Russian Academy of Sciences,
Nab. Makarova, 2, Saint Petersburg, 199034, Russia

³Helmholtz-Zentrum Berlin für Materialien und Energie GmbH, BENSC,
Glienicke St., 14109 Berlin, Germany

⁴Saint Petersburg State Polytechnical University,
Polytkhnicheskaya 29, 195251, Saint Petersburg, Russia

*Corresponding author: alex.nabereznov@mail.ioffe.ru

Microscopic structure of three types of porous glasses with the average pore diameter of 5, 7 and 140 nm obtained by chemical etching was studied by neutron diffraction. The analysis of diffraction patterns has shown that in these glasses, besides an amorphous phase forming a weakly structured background, there are microscopic crystalline inclusions of sassolite with a diffraction size of 26 ± 3 nm and of α -quartz with a characteristic size of 6 ± 1 nm. Microcrystalline inclusions sizes do not depend on the average pore size diameter. It is shown that in these samples a tridymite phase does not make a significant contribution to observed scattering and a relative sassolite contribution decreases substantially with the average pore size increasing from 5 to 140 nm.

Keywords: porous borosilicate glass, neutron diffraction, nanoparticles.

1. Introduction

Porous glasses (PG), obtained as a result of through chemical etching of alkali borosilicate (ABS) glasses with a two-framework structure [1, 2], are promising prototype matrices for new nanocomposite materials (NCM), whose properties are defined by the properties and the state of substances embedded into nano-range pore space [3]. In these NCM, numerous interesting, and absent in bulk, macroscopic physical properties (both from fundamental viewpoint and practical application) have been observed. Thus, for example, for nanostructured sodium nitrite (obtained by embedding the matrices with different average pore diameters into porous glasses) it is shown that a decreasing pore diameter leads to a decrease in the temperature of phase

transition (PT) into a ferroelectric phase, type of PT, giant growth of dielectric permittivity and mobility of constituent ions above PT temperature [4–7]. These NCMs with embedded ferroelectrics could be considered as quite promising materials for FeRAM [8] and capacitors with ultra-high capacitance.

While studying the temperature evolution of NCM crystal structure and determination of nanoclusters size, it is important to have information about a possible contribution from the matrix itself (porous glass) to the diffraction peaks observed in the experiment. Using X-ray scattering on porous glasses, it is shown that depending on the composition of initial two-phase ABS glasses, the obtained PG are either X-ray amorphous [9] or they also contain microscopic crystalline α -quartz, tridymite and sassolite inclusions besides amorphous silica [10]. It should be noted that the presence of small amounts of microcrystalline boron- and silica-containing phases with compositions depending on initial glasses chemical etching conditions was established by electron microdiffraction [11, 12]. The positions of elastic peaks corresponding to these inclusions can coincide with the positions of reflections from the embedded material, and this will lead to distortion of not only a peak shape and broadening of Bragg peaks, but also to incorrect results related to crystal structure and nanoclusters sizes of embedded materials.

To determine this possible contribution from the microcrystallites of the matrix itself and to estimate also the sizes of these microcrystallites, the study of the structure of three porous glasses types was carried out using neutron diffraction. The advantages of this method in comparison with those mentioned above are: *i*) this is a nondestructive method, *ii*) neutron penetration in samples is large (many orders of magnitude larger in comparison with X-rays), which allows to obtain a diffraction pattern corresponding to the total in-beam volume averaging, *iii*) at the same time there are no limitations in the X-ray phase analysis: a small amount (< 5%) of crystalline phase or small crystallite sizes lead to diffraction peaks broadening that makes it impossible to give an unambiguous answer about the presence of microcrystallites. Electron microdiffraction allows to register the presence of a microcrystalline phase, but its identification is complicated in those cases when there are more than two microcrystalline phases. In a number of cases, neutron diffraction allows to realize this procedure.

2. Samples and experiments

Three porous glasses types, PG5, PG7 and PG140 with the average pore diameters of 5, 7 and 140 nm, respectively, were used as samples. PG compositions and parameters characterizing the pore space are listed in Table 1. According to Zhdanov's definition [1], PG5 and PG7 are microporous glasses. A system of interconnected open-ended pores in these PGs is obtained after a single etching cycle of two-phase ABS glasses by acid-salt solution. According to the results of an initial glasses structure study by transmitted electron microscopy (TEM), the sizes of liquation channels in the investigated two-phase glasses range from 25–60 nm to ~200 nm [9, 11, 15, 16].

Table 1. Compositions of porous glasses and parameters of pore space.

	Porous glass composition [wt%]						Pore space parameters	
	Na ₂ O	B ₂ O ₃	SiO ₂	Al ₂ O ₃	P ₂ O ₅	F	Average pore radius* [nm]	Porosity** [%]
PG5	0.17	5.96	93.75	≤ 0.1	0.07	0.05	4.9	27
PG7	0.43	5.80	93.67	≤ 0.1	–	–	7.1	25
PG140	0.60	8.62	90.55	0.23	–	–	140	57

Note: for PG5 glass, the data from [13, 14] are listed.

We have defined pores parameters for PG7 and PG140 according to the procedure explained in [13]:

*Calculation from nitrogen thermal desorption;

**From weight method.

It should be noted that there is a difference between the microporous glasses PG5 and PG7, which consists in their qualitative composition (ref. Table 1), and in particular there are phosphate- and fluoride-ions in PG5.

As for PG140, this macroporous glass (according to Zhdanov's definitions [1]) was obtained from microporous glass (like PG7) after the second chemical etching cycle, but by alkali solution. As a result of one-stage glasses chemical etching, the parameters of PG pore space are determined by the sizes of the so-called secondary silica particles and the density of their package [17]. Pore diameters of macroporous glasses correspond to liquation channels sizes, formed by a chemically unstable phase in the initial two-phase glass [18].

After chemical etching of glasses, the alkali and acid residuals were carefully washed out from PG by distilled water. Directly before measurements all samples were dried in a vacuum furnace at ~150 °C during approximately 1.5 days to remove water adsorbed in pores and to decrease the background due to neutron scattering on hydrogen at diffraction measurements. All experiments were carried out on a powder diffractometer E2 (Helmholtz-Zentrum Berlin, Germany) at incident neutrons wavelength 1.21 Å and at scattering angle 2θ from 6 to 82°.

3. Results and discussion

In Figure 1, the experimental diffraction patterns for glasses PG5, PG7 and PG140 are presented. It can be easily seen that in addition to a large background associated with scattering on amorphous silica there are also clearly pronounced diffraction peaks (marked with arrows and numbers 1–5), which indicate the presence of regions with crystal structure, and their total contribution to the scattering is quite large in comparison with a background. Widths of these peaks considerably exceed the experimental resolution of a diffractometer. It is easy to see that the integral intensity of the first peak decreases with pore diameter increasing and the peak itself becomes less pronounced. It should be noted that for PG7 and PG140 practically identical diffraction patterns are observed, which is probably caused by the same silica framework nature.

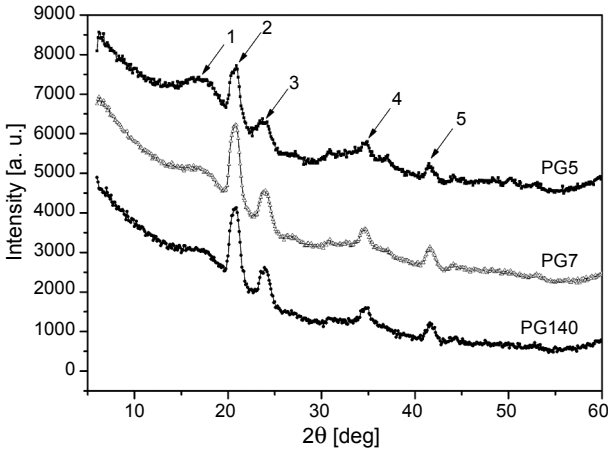


Fig. 1. Neutron diffraction spectra from porous glasses with the average pore diameter of 5 nm (PG5), 7 nm (PG7) and 140 nm (PG140). Numbers 1–5 mark the positions of peaks used to determine parameters of phases contained in these glasses. For obviousness sake spectra shifted on y-axis by 1000.

Some difference between PG5 and PG7 (PG140) diffraction patterns can be caused by formation (along with borosilicate microcrystalline phases) of the phosphorous- and/or fluoride-containing crystal structures, like for example Na_2SiF_6 [19]. Unfortunately, the number of peaks available, their apparent broadening and high background do not allow us to carry out a full scale profile analysis procedure to determine all possible contributions to the total diffraction pattern from different phases; however available experimental data allows to make a whole number of conclusions important for understanding the microscopic structure of porous glasses.

Initially we have tried to identify crystalline phases giving a contribution into the scattering. To this end, the expected neutron scattering spectra have been modelled tridymite, α -quartz and sassolite, which presence in similar glasses have been shown in [9–12]. Necessary unit cell parameters and atoms positions have been taken from papers [20–22]. In Figure 2, the calculated spectrum for tridymite and the experimental spectrum for PG140 are shown. As it is possible to see, the positions of very intensive peaks (especially at angles 17–23°) for tridymite do not coincide with experimental peaks, moreover there are almost no tridymite peaks in the region where experimental elastic peaks are observed.

It leads to the conclusion that the contribution of a tridymite phase is too small or is absent practically. Therefore this contribution to the scattering was not further considered. In Figure 3 the calculated spectra for α -quartz (Fig. 3a) and sassolite (Fig. 3b) in comparison with experimental data for PG7 are presented. It is easy to see that there is almost no contribution from α -quartz to peaks 3, 4 and 5 since the elastic peaks corresponding to this quartz modification lie at different diffraction angles. However, there are peaks corresponding to sassolite structure. For peaks 1 and 2

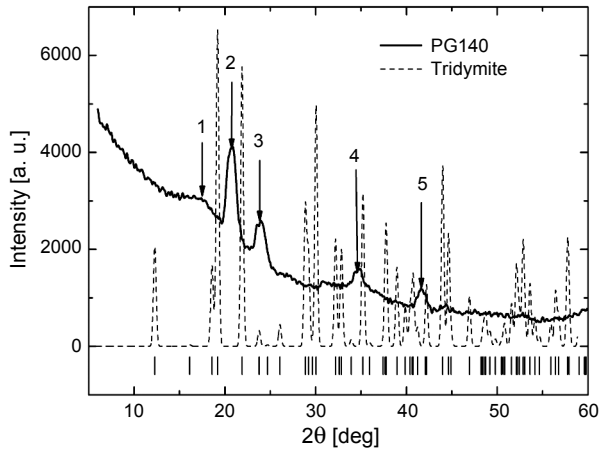


Fig. 2. Experimental spectrum for PG140 and calculated spectrum (corrected for diffractometer resolution) for tridymite phase (dashed line). Vertical lines at the bottom – tridymite elastic peaks positions.

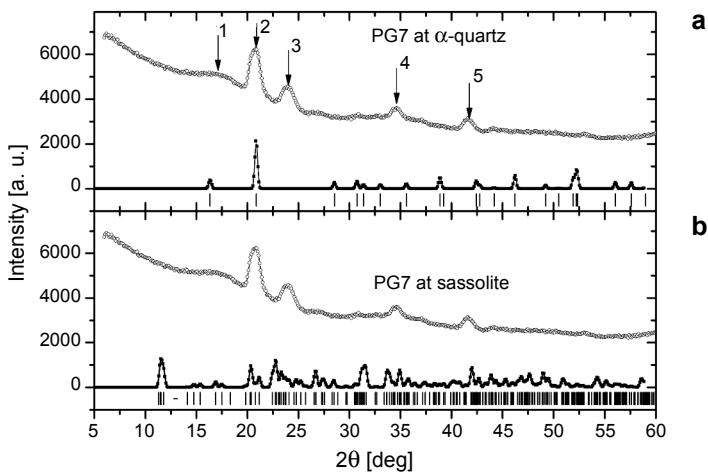


Fig. 3. Experimental spectrum for PG7 and calculated ones for α -quartz (a) and sassolite (b) adjusted for instrumental resolution. Vertical lines at the bottom – elastic peaks position for the respective phases.

the situation is a bit different: in these angle diapasons there are peaks both from α -quartz and sassolite. It is known that the intensity of scattering for every Bragg reflection is proportional to a structure factor in square F^2 .

In the first step of the treatment, peak 3 of an experimental pattern has been represented by a sum of Gaussians (this shape corresponds to an instrumental line shape of our instrument) corresponding to elastic reflection for sassolite in this angle diapason. The amplitude of each Gaussian was determined by the corresponding

T a b l e 2. *HKL* values, peaks positions (scattering angle) and structure factors for sassolite elastic peaks in peak 3 angle range of diffraction pattern (Figs. 1–3).

Reflection number	<i>HKL</i>	Reflection multiplicity	Scattering angle 2θ [deg]	Structure factor F^2
1	[1–21]	2	22.45	12.34
2	[002]	2	22.76	19.56
3	[–102]	2	22.83	7.16
4	[–121]	2	23.32	14.13
5	[200]	2	23.7	8.22
6	[0–21]	2	24.07	7.86
7	[–221]	2	24.78	8.73
8	[2–11]	2	25.22	7.53

structure factor (Miller indices *HKL*, scattering angles and structure factors are presented in Tab. 2), fitting parameters (except background parameters) were Gaussian widths, which for all peaks were the same (since its value is determined by convolution of instrumental resolution with peak broadening due to a finite crystallite size), and a parameter taking into account a normalization on integral intensity under that peak. The obtained curves described the shape of peak 3 quite well for all data. Using calculated standard deviation value σ , the full width at half maximum (FWHM) B_{exp} was determined and then the broadening due to a size effect was found using a standard formula

$$B_{\text{size}} = \sqrt{B_{\text{exp}}^2 - B_{\text{res}}^2} \quad (1)$$

the instrumental FWHM B_{res} in this angles range was known initially from E2 diffractometer calibration on standard samples. Then from B_{size} a respective crystallite size was determined using a well-know Scherrer's formula [23]:

$$s = \frac{0.9\lambda}{B_{\text{size}} \cos(\theta)} \quad (2)$$

where: λ – neutron wavelength, B_{size} – experimental broadening of elastic peak, θ – scattering angle.

Using this approach, we have obtained the estimation of a sassolite nanocluster size 26 ± 3 nm. It should be noted that the sizes (diameters) of liquation channels in the initial two-phase glasses allow the formation of sassolite nanoparticles of this size in pore space. Further this value was used to describe the contribution in scattering from these nanoclusters to all other peaks, where it is present (peaks 1, 4 and 5) together with α -quartz, and for determination of α -quartz nanoparticles size from peak 2 also. Using the calculation procedure mentioned above and taking into account the de-

pendence of diffractometer resolution function from scattering angle, it is possible to achieve a fine fit for shapes of peaks 4 and 5 and satisfactory fit for peak 1. Unfortunately, peak 1 contains the contributions not only from α -quartz but possibly from a tridymite phase. Moreover, the sharp growth of a background at small angles is difficult to be correctly approximated. The last two circumstances and insufficient statistics have not permitted to determine the true shape of peak 1. At the next step, the similar procedure (formula (3)) was applied for peak 2 for all obtained diffraction patterns, as there were the contributions from both sassolite and α -quartz phases into the integral intensity (and line-shape) of this peak;

$$I \sim A \sum F_i^2 \exp \left[-\frac{(x - x_i)^2}{2\sigma_1^2} \right] + B \sum F_j^2 \exp \left[-\frac{(x - x_j)^2}{2\sigma_2^2} \right] \quad (3)$$

where: I – integral intensity under peak 2, F_i^2 – structure factors for α -quartz reflections; F_j^2 – structure factors for sassolite reflections; x_i and x_j – elastic peaks positions for α -quartz and sassolite from simulation data; σ_1 and σ_2 – elastic widths of α -quartz and sassolite peaks, respectively. The value σ_2 was taken from fitting of peak 3 and was constant at fitting of peak 2; varied parameters were A , B and σ_1 – width of α -quartz reflections. The parameters A and B correspond to the relative α -quartz and sassolite phases contributions. The peak positions and structure factors for bulk α -quartz and sassolite used at simulation are listed in Tab. 3.

Table 3. HKL values, peaks positions (scattering angle) and structure factors for α -quartz and sassolite elastic peaks in peak 2 angle range of diffraction pattern (Figs. 1–3).

Substance	HKL	Reflection multiplicity	Scattering angle 2θ [deg]	Structure factor F^2
α -quartz	[011]	6	20.8533	3.5
α -quartz	[101]	6	20.8533	9.86
Sassolite	[2–10]	2	20.27	6.77
Sassolite	[110]	2	20.37	11.21
Sassolite	[–111]	2	20.78	3.09
Sassolite	[–211]	2	21.16	8.5

The results of fitting procedure of peak 2 for all glass types are shown in Fig. 4. One can see that the description of experimental shape is very good. From the broadening of α -quartz elastic peaks, the size of α -quartz nanocrystals was determined to be 6 ± 1 nm and this size does not depend practically on glass type. The obtained A and B parameters are presented in Tab. 4. It can be seen that with an increasing average pore diameter, the relative contribution of α -quartz phase to the total scattering (A/B ratio) increases and sassolite fraction is determined with larger relative error.

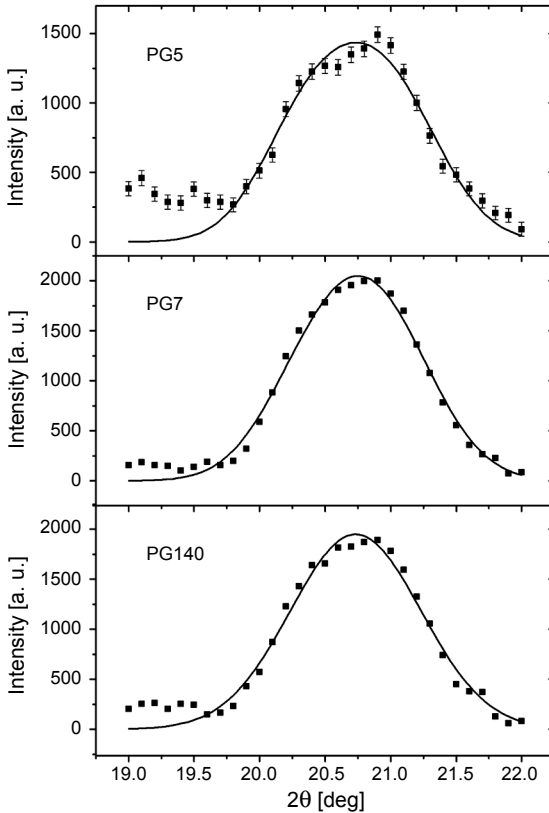


Fig. 4. Results of the integral intensity and peak shape fitting for peak 2 for PG5, PG7 and PG140 using the model described in the text. Experimental errors are shown in the figure.

T a b l e 4. Parameters A and B values (Eq. (3)) corresponding to relative contribution from α -quartz and sassolite to peak 2 integral intensity for PG5 and PG140.

Average pore diameter [nm]	Parameter A (α -quartz)	Parameter B (sassolite)	Ration A/B
5	86 ± 2	21 ± 2	4.1 ± 0.5
140	138 ± 7	17 ± 6	8.1 ± 3.2

A decreasing of sassolite contribution in the scattering at transition from microporous (PG5) to macroporous (PG140) glasses can be related to a decrease in sassolite concentration (on absolute scale) due to the dissolution of the boron-enriched inner surface layer of pore walls at alkali etching of PG [24].

4. Conclusions

The studies of the microstructure of porous glasses with average pore diameters of 5, 7 and 140 nm by neutron diffraction have shown that in these glasses there are sassolite

and α -quartz microcrystallites with characteristic size of 26 ± 3 nm and 6 ± 1 nm, respectively. Their sizes are independent of pore diameters. A significant contribution of a tridymite phase in our studies is not found. It is shown that the sassolite contribution decreases substantially with an increase in the average pore diameter.

Acknowledgments – This work was supported by the Russian Foundation for Basic Research (projects 11-03-00747, 09-02-00329, 11-02-00739) and the Department of Chemistry and Material Science of the Russian Academy of Sciences (project PFI OXNM-02 PAN). The authors would like to thank the colleagues from the Laboratory of Physical Chemistry of Glasses ISC RAS T.G. Kostyrev, L.A. Doronina and L.F. Dikaya for carrying out the chemical analysis of glasses.

References

- [1] ZHDANOV S.P., *Porous glasses and their structure*, Wissenschaftliche Zeitschrift der Friedrich-Schiller-Universität Jena. Mathematisch-Naturwissenschaftliche Reihe, 1987, pp. 817–830.
- [2] MAZURIN O.V., ROSKOVA G.P., AVERYANOV V.I., ANTROPOVA T.V., *Two-Phase Glasses Structure, Properties, Application*, Nauka, Leningrad, 1991, Chapter 10, p. 276, (in Russian).
- [3] ENKE D., JANOWSKI F., SCHWIEGER W., *Porous glasses in the 21st century – A short review*, Microporous and Mesoporous Materials **60**(1–3), 2003, pp. 19–30.
- [4] FOKIN A.V., KUMZEROV YU.A., OKUNEVA N.M., NABEREZHNOV A.A., VAKHRUSHEV S.B., GOLOSOVSKY I.V., KURBAKOV A.I., *Temperature evolution of sodium nitrite structure in a restricted geometry*, Physical Review Letters **89**(17), 2002, article 175503.
- [5] VAKHRUSHEV S.B., KUMZEROV YU.A., FOKIN A., NABEREZHNOV A.A., ZALAR B., LEBAR A., BLINC R., *^{23}Na spin-lattice relaxation of sodium nitrite in confined geometry*, Physical Review B **70**(13), 2004, article 132102.
- [6] VAKHRUSHEV S.B., KOROLEVA E.YU., KUMZEROV YU.A., NABEREZHNOV A.A., FOKIN A.V., KOROTKOV L.H., TOVAR M., COLLA E.V., *Structure and properties of sodium nitrite in restricted geometry*, Nanotekhnika **1**(5), 2006, pp. 18–24, (in Russian).
- [7] VAKHRUSHEV S.B., GOLOSOVSKY I.V., KOROLEVA E.YU., NABEREZHNOV A.A., OKUNEVA N.M., SMIRNOV O.P., FOKIN A.V., TOVAR M., GLAZMAN M., *Structure and dielectric response of $\text{Na}_{1-x}\text{K}_x\text{NO}_2$ nanocomposite solid solutions*, Physics of the Solid State **50**(8), 2008, pp. 1548–1554.
- [8] ARAUJO C., SCOTT J.F., BRUCE GODFREY R., McMILLAN L., *Analysis of switching transients in KNO_3 ferroelectric memories*, Applied Physics Letters **48**(21), 1986, pp. 1439–1440.
- [9] ANTROPOVA T.V., DROZDOVA I.A., *Electron-microscopy and microdiffraction study of porous glasses*, Russian Journal of Applied Chemistry **66**(10), 1993, pp. 1675–1684.
- [10] ANTROPOVA T.V., TSYGANOVA T.A., ROSKOVA G.P., KOSTYREVA I.G., POLYAKOVA I.G., MEDVEDEVA S.V., *Some features of leaching of two-phase alkali borosilicate glass containing PbO* , Glass Physics and Chemistry **27**(2), 2001, pp. 175–181.
- [11] ANTROPOVA T.V., DROZDOVA I.A., *Influence of synthesis conditions of porous glasses on their structure*, Fizika i Khimiya Stekla **21**(2), 1995, pp. 131–140, (in Russian).
- [12] ANTROPOVA T.V., DROZDOVA I.A., YASTREBOV S.G., EVSTRAPOV A.A., *Porous glass: Inhomogeneities and light transmission*, Optica Applicata **30**(4), 2000, pp. 553–567.
- [13] ANTROPOVA T.V., ANFIMOVA I.N., GOLOVINA G.F., *Influence of the composition and temperature of heat treatment of porous glasses on their structure and light transmission in the visible spectral range*, Glass Physics and Chemistry **35**(6), 2009, pp. 572–579.
- [14] ANTROPOVA T.V., DROZDOVA I.A., VASILEVSKAYA T.N., VOLKOVA A.V., ERMAKOVA L.E., SIDOROVA M.P., *Structural transformations in thermally modified porous glasses*, Glass Physics and Chemistry **33**(2), 2007, pp. 109–121.
- [15] GUTINA A., ANTROPOVA T., RYSIAKIEWICZ-PASEK E., VIRNIK K., FELDMAN YU., *Dielectric relaxation in porous glasses*, Microporous and Mesoporous Materials **58**(3), 2003, pp. 237–254.

- [16] ANTROPOVA T.V., DROZDOVA I., KUKHTEVICH I., EVSTRAPOV A., ESIKOVA N., *Application of high resolution microscopy and optical spectroscopy for study of phase separation in phosphorus- and fluorine-containing sodium borosilicate glasses*, *Optica Applicata* **40**(2), 2010, pp. 293–304.
- [17] KREISBERG V.A., RAKCHEEV V.P., ANTROPOVA T.V., *Influence of the acid concentration on the morphology of micropores and mesopores in porous glasses*, *Glass Physics and Chemistry* **32**(6), 2006, pp. 615–622.
- [18] BURKAT T.M., DOBYCHIN D.P., *Macrokinetics of porous alkali leaching*, *Soviet Journal of Glass Physics and Chemistry* **18**(2), 1992, pp. 165–170.
- [19] DROZDOVA I., ANTROPOVA T., *Features of a structure of the phase-separated and porous borosilicate glasses with/without an impurity of fluorid-ions according to electron microscopy*, *Optica Applicata* **38**(1), 2008, pp. 17–24.
- [20] BOISEN M. B., GIBBS G.V., BUKOWINSKI M.S.T., *Framework silica structures generated using simulated annealing with a potential energy function based on an $H_6Si_2O_7$ molecule*, *Physics and Chemistry of Minerals* **21**(5), 1994, pp. 269–284.
- [21] GAJHEDE M., LARSEN S., RETTRUP S., *Electron density of orthoboric acid determined by X-ray diffraction at 105 K and ab initio calculations*, *Acta Crystallographica Section B* **42**(6), 1986, pp. 545–552.
- [22] WILL G., BELLOTTO M., PARRISH W., HART M., *Crystal structures of quartz and magnesium germanate by profile analysis of synchrotron-radiation high-resolution powder data*, *Journal of Applied Crystallography* **21**(2), 1988, pp. 182–191.
- [23] PATTERSON A.L., *The Scherrer formula for X-rays particle size determination*, *Physical Review* **56**(10), 1939, pp. 978–982.
- [24] BURKAT T.M., DOBYCHIN D.P., *Distribution of boron oxide in surface layer of porous glasses*, *Fizika i Khimya Stekla* **17**(1), 1991, pp. 160–163, (in Russian).

Received September 30, 2011